

# EVALUATION OF PASSIVATION SCHEMES OF LARGE AREA SI SOLAR CELLS: SEPARATING SERIAL RESISTANCE FROM OTHER LOSSES BY THE CELLO TECHNIQUE

Andreas Schütt<sup>1</sup>, Jürgen Carstensen<sup>1</sup> Helmut Föll<sup>1</sup>

Sinje Keipert-Colberg<sup>2</sup>, Dietmar Borchert<sup>2</sup>

<sup>1</sup>: Institute for Materials Science, Faculty of Engineering, Christian-Albrechts-University Kiel, Kaiserstr. 2, 24143 Kiel, Germany;

contact: Andreas Schütt, asc@tf.uni-kiel.de, phone: +49 431 880-6181 FAX -6178;

<sup>2</sup>: Fraunhofer Institute for Solar Energy Systems, Laboratory and Servicecenter Gelsenkirchen, Auf der Reihe 2, 45884 Gelsenkirchen, Germany

**ABSTRACT:** Solar cells with an inhomogeneous distribution of high  $R_{ser}$  are not well described by the standard  $I-V$  curve model. On such solar cells process optimization for improving the front surface passivation can not be monitored by  $I-V$  curve analysis. Therefore in this paper local CELLO maps are used instead of integral  $I-V$  curve data to benchmark different cleaning procedures. The CELLO technique allows the determination of solar cell parameters ( $\tau_{life}$ ,  $R_{ser}$ ,  $R_{shunt}$ ) *locally* and *non-destructively* by analyzing the current ( $dI$ ) or voltage ( $dU$ ) response of a globally illuminated solar cell (0.3 suns) to a local perturbation induced with a LASER beam. CELLO  $R_{ser}$  maps are used to identify loss areas due to a high  $R_{ser}$  and to dismiss cells where losses are dominated by  $R_{ser}$ . CELLO maps taken at the maximum power point (mpp) are used for a qualitative (and quantitative) analysis of (local and global) efficiency losses. Further defects like surface damages, scratches or inhomogeneous SiN areas are identified by comparing CELLO power loss maps with optical microscope images. From  $dU_{mpp}(x,y)/dI_{sc}(x,y)$  maps a relative gain of 20 % for optimal cleaning was found.

Keywords: Passivation, Etching, Characterization

## 1 INTRODUCTION

The main factors limiting the efficiency of large-area Si solar cells are lifetime ( $\tau_{life}$ ), series resistances ( $R_{ser}$ ), and shunts ( $R_{shunt}$ ), but also additional factors like front surface recombination velocity  $S_f$  have to be optimal for high-efficiency solar cells [1, 2]. Separating the problems caused by the main limiting factors from the problems caused by other loss factors is often very difficult. To that end, usually processing and characterization of a huge number of cells is carried out to get relevant information just from a large statistics. So the success of extracting information about process-induced losses depends on the number of processed cells (high costs) and the variance of the main limiting factors.

On the other hand, CELLO measurements reliably allow to calculate serial resistance  $R_{ser}$  maps [3, 4] and to estimate the efficiency losses of a solar cell (both qualitatively and quantitatively) [5].

In this paper different chemical cleaning procedures prior to the PECVD SiN deposition [1, 2] are analyzed for the optimization of standard p-type Si solar cells. Standard  $I-V$  curve measurements, CELLO maps, and optical microscope images are compared and combined for characterizing  $S_f$ . The local  $R_{ser}$  information from CELLO maps allows to identify statistical outliers (e.g. processing errors like failed screen printing process) and to pre-select all cells useful for quantifying the efficiency of the chemical cleaning steps.

## 2 SAMPLE PREPARATION

More than 100 multicrystalline Si solar cells are produced by a standard Si solar cell process (cf. Fig. 1). Intentionally the quality of the front surface passivation is varied by applying different surface cleaning procedures prior to the SiN PECVD deposition step (cf. Table 1). According to Angermann [2] these treatments should induce different levels of interface state density  $D_{it}$ , and a higher  $D_{it}$  will in turn increase the recombination at the interface and thus increase  $S_f$ , which

will be checked in this study. For optimization of the firing temperature 2-3 different peak firing temperatures for identically processed solar cells are used. 20 cells of neighboring wafers (cf. wafer number) are characterized by CELLO measurements in order to evaluate the passivation quality of the different cleaning procedures.

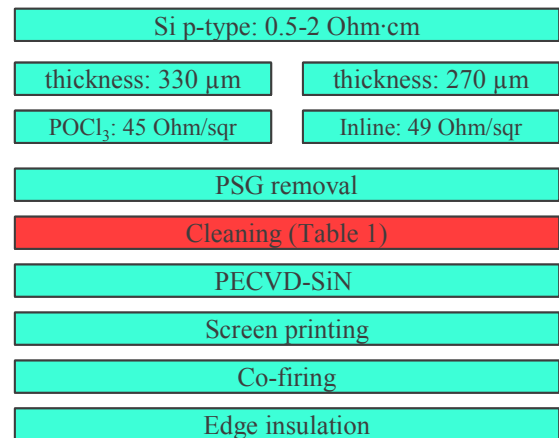


**Fig. 1:** Solar cell processing scheme

## 3 CHARACTERIZATION OF SOLAR CELLS

As already stated in [1] standard  $I-V$  curve measurements did not allow a consistent analysis of the efficiency of the above-described variations in the cleaning steps, which is mainly due to a large variation in the quality of the contact resistance. Using the  $I-V$  curve data the 20 most promising candidates out of more than 100 cells have been analyzed extensively by CELLO measurements. For a further subset of cells which showed the most homogeneous CELLO maps a detailed comparison of the remaining defects in the maps with optical microscope images has been performed.

| Name                       | Step 1                                   | Step 2                   | Step 3                                   | Step 4                   | Step 5                                   | Total oxidation time | Final HF Dip | $D_{it}$  |
|----------------------------|--|--------------------------|--|--------------------------|--|----------------------|--------------|-----------|
| HNO <sub>3</sub><br>4 min  | 2 min<br>HNO <sub>3</sub> 69 %,<br>25°C  | 1 min<br>HF 1 %,<br>25°C | 2 min<br>HNO <sub>3</sub> 69 %,<br>25°C  |                          |  | 4 min                | No           | very high |
| HNO <sub>3</sub><br>20 min | 10 min<br>HNO <sub>3</sub> 69 %,<br>25°C | 1 min<br>HF 1 %,<br>25°C | 10 min<br>HNO <sub>3</sub> 69 %,<br>25°C |                          |  | 20 min               | No           | high      |
| HNO <sub>3</sub><br>30 min | 10 min<br>HNO <sub>3</sub> 69 %,<br>75°C | 1 min<br>HF 1 %,<br>25°C | 10 min<br>HNO <sub>3</sub> 69 %,<br>75°C | 1 min<br>HF 1 %,<br>25°C | 10 min<br>HNO <sub>3</sub> 69 %,<br>75°C | 30 min               | No           | middle    |
| RCA+HF                     | 10 min<br>RCA 1,<br>80-85°C              | 15 s<br>HF 1 %,<br>25°C  | 10 min<br>RCA 2,<br>80-85°C              | 15 s<br>HF 1 %,<br>25°C  |  | 20 min               | Yes          | low       |
| HNO <sub>3</sub> +HF       | 10 min<br>HNO <sub>3</sub> 69 %,<br>25°C | 1 min<br>HF 1 %,<br>25°C | 10 min<br>HNO <sub>3</sub> 69 %,<br>25°C | 1 min<br>HF 1 %,<br>25°C |  | 20 min               | Yes          | low       |
| HF                         |  | 1 min<br>HF 1 %,<br>25°C |  |                          |  |                      | Yes          | low       |

**Table 1:**  $D_{it}$  variation by different surface cleaning procedures prior to PECVD SiN deposition. Between every step a DI water rinse is performed.

Potentiostatic ( $dI$ ) and galvanostatic ( $dU$ ) CELLO maps along the  $I$ - $V$  curve [short circuit (sc); maximum power point (mpp); open circuit (oc)] under 0.3 sun global illumination have been measured for all 20 cells using a laser wavelength of 830 nm (light penetration depth of  $\sim 20$   $\mu$ m) and with a lock-in frequency of 6 kHz. Several serial resistance ( $R_{ser}$ ) maps derived from  $dI_{sc}$  maps,  $dU_{oc}$  maps, and the  $I$ - $V$  curve [3] are shown in the first column in Fig. 2 and Fig. 3. Red colors mark areas with higher serial resistances. All cells with a large area fraction of high serial resistances have been ruled out and are not analyzed further, i.e. only those firing and cleaning conditions have been taken into account which allow to obtain a low contact resistance and thus reasonably high solar cell efficiencies. A selection of these solar cells is given in Figs. 2 and 3. Note that within each column the same limits for the histograms have been used. Cell \_167 of Fig. 2 is an example of an excluded cell, all other are the remaining cells with best contact resistances.

Additionally the ratios of ( $dI_{mpp} / dI_{sc}$ ) and ( $dU_{mpp} / dI_{sc}$ ) are presented in Fig. 2 and Fig 3 in the second and third column. Here the dark regions indicate areas of larger power losses [5]. The clear anticorrelation, e.g. for the cells \_164 and \_158, between the  $R_{ser}$  maps and the losses in ( $dI_{mpp} / dI_{sc}$ ) resp. ( $dU_{mpp} / dI_{sc}$ ) again reflect the result extracted from the  $I$ - $V$  curves, namely, that many cells of this study are limited by high serial resistances (high contact resistances).

Since all maps within one column have the same scaling it is quite obvious that the variation in the cleaning procedures does not have a significant influence on the ( $dI_{mpp} / dI_{sc}$ ) maps. The same is true for the short circuit current maps  $dI_{sc}$  (not shown here). A detailed analysis of the serial resistance maps  $R_{ser}$  leads to the assumption that there is probably a correlation to the cleaning steps as well, but since definitely several statistical outliers exist which independently of the cleaning process showed a large lateral variation in the serial resistance all these cells have been excluded from further analysis as mentioned before.

In contrast to the other maps, ( $dU_{mpp} / dI_{sc}$ ) maps show a clear correlation to the cleaning procedures with respect to the average value and to some extent in the lateral variation of the data. Especially *all* cells with “final HF dip” show the largest average values and the least lateral variation in the ( $dU_{mpp} / dI_{sc}$ ) maps. This is a clear indication that these maps are sensitive to the surface passivation and will thus be used for a short further discussion of the influence of the various cleaning steps on ( $dU_{mpp} / dI_{sc}$ ) maps and consequently on the solar cell efficiency.

For the cells with a final HF dip, systematically better results are found for those with a POCl<sub>3</sub> diffusion in comparison to those with the inline diffusion (cell\_158 vs. cell\_130).

For most cells without HF dip, the areas with high dislocation densities are clearly visible in the ( $dU_{mpp} / dI_{sc}$ ) maps as regions with higher losses; e.g. the central area of cell \_160 shows large losses while for the neighboring cell \_158 with HF dip no losses in this region are found. This illustrates the importance of proper surface cleaning especially on multicrystalline Si material.

A second variation that only the cells without HF dip are sensitive to is the oxidation time for removing material from the emitter; a longer total oxidation time (cf. Table 1) improves significantly the ( $dU_{mpp} / dI_{sc}$ ) maps (cf. \_160, \_164, \_166). These results are in good agreement with the discussion by Angermann [2] that an HF dip prior to SiN deposition causes a good chemical passivation of dangling bonds and thus reduces  $D_{it}$  and improves the surface recombination velocity at the front side  $S_f$  – which the CELLO ( $dU_{mpp} / dI_{sc}$ ) maps are sensitive to. According to [2] one mayor effect reducing  $D_{it}$  is a smaller surface roughness. This can explain the improvements found for an increased oxidation time on the cells (cf. \_160, \_164, \_166); of course this procedure will lead to smoother surfaces.

In summary the HF dip just leads to a much more robust surface passivation reducing the effects of otherwise relevant changes in the production scheme.

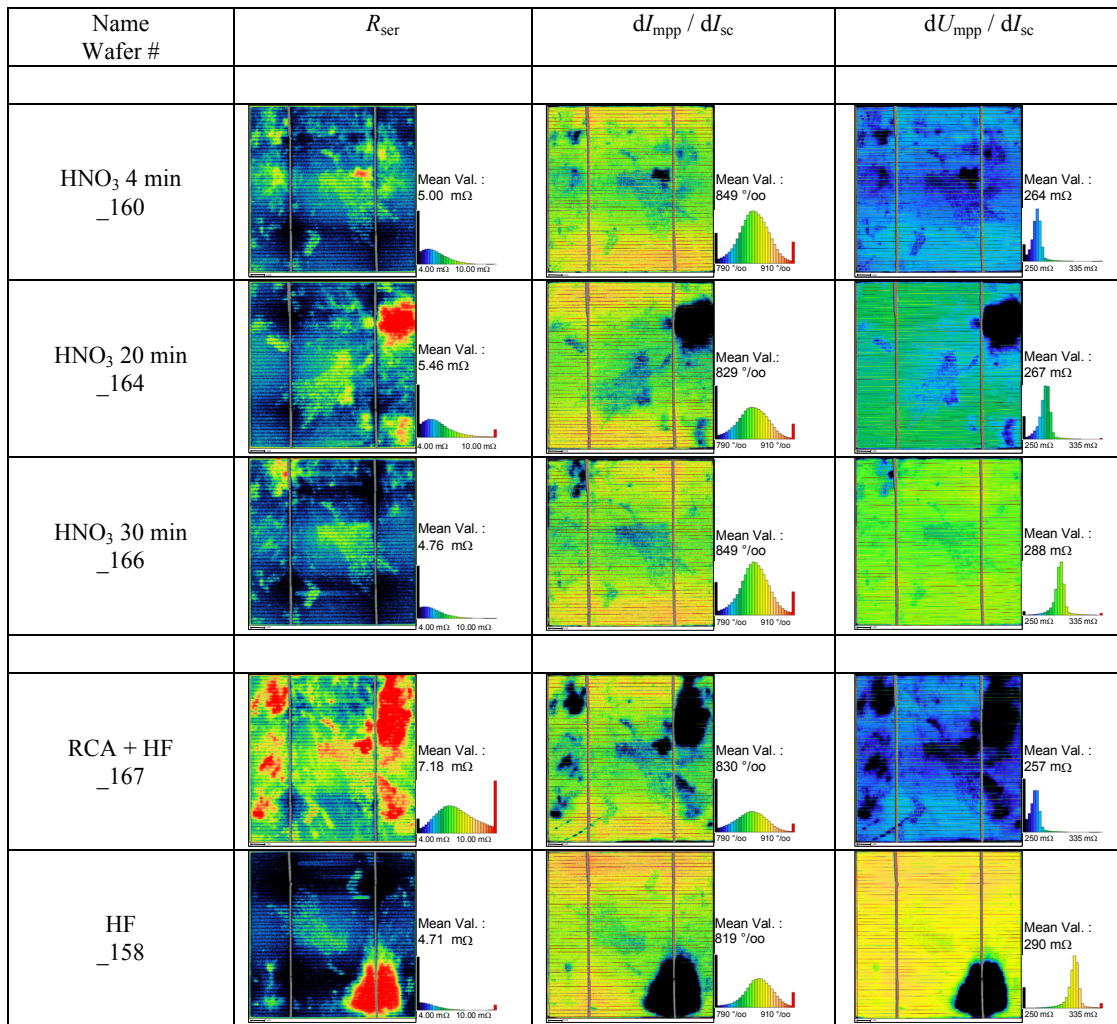


Fig. 2: Inline diffusion cells

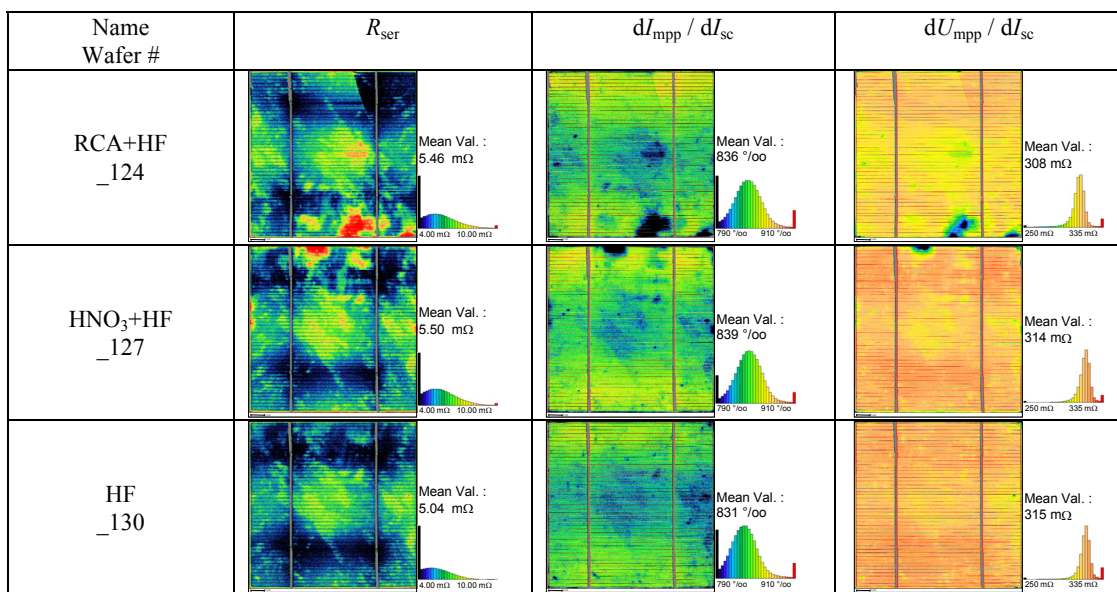


Fig. 3: POCl<sub>3</sub> diffusion cells

Finally the remaining local losses visible in the  $(dU_{\text{mpp}} / dI_{\text{sc}})$  maps in Fig. 3 for the best solar cells are investigated. One example is highlighted in Fig. 4 for cell \_130. The area with the largest losses has been re-measured with CELLO using a much higher spatial resolution showing strong local losses and a surrounding transient area with continuously decreasing losses. In the optical microscope at exactly this position a partial penetration of the SiN layer and most probably the p-n junction as well has been found. Such defects are well-known to locally shunt a solar cell [6]. Using the same approach on other positions with increased  $(dU_{\text{mpp}} / dI_{\text{sc}})$  values microcracks, surface scratches, and more defects in the SiN coating have been identified. All of these defects were found in the  $(dI_{\text{mpp}} / dI_{\text{sc}})$  maps as well. None of these defects was induced by the cleaning or could have been eliminated using an improved cleaning procedure.

Using the approach described in [4] relative efficiency losses can be estimated from  $(dU_{\text{mpp}} / dI_{\text{sc}})$  maps. Comparing cells like \_130 (lowest  $D_{\text{it}}$ ) and \_160 (highest  $D_{\text{it}}$ ) a relative improvement of 20 % has been found for the optimal cleaning procedure from this local analysis which before was hidden in the global  $I$ - $V$  data of the more than 100 solar cells produced.

#### 4 SUMMARY

Using CELLO maps for the pre-selection of cells with small  $R_{\text{ser}}$  (by excluding high  $R_{\text{ser}}$  processing defects and over- and underfired cells) allows to extract information about the quality of surface passivation which was not accessible from statistical analysis of global  $I$ - $V$  curve data.

This pre-selection approach automatically excludes surface passivation schemes from the evaluation that do not result in a good contact resistance. Best passivation results have been found for an HF dip prior to the SiN deposition. Optical microscope analysis on the solar cells with optimal cleaning showed that none of the defects on these cells was related to cleaning. A relative efficiency gain  $\sim 20$  % due to the proper cleaning was hidden in the global  $I$ - $V$  curve data but could be extracted from local CELLO maps.

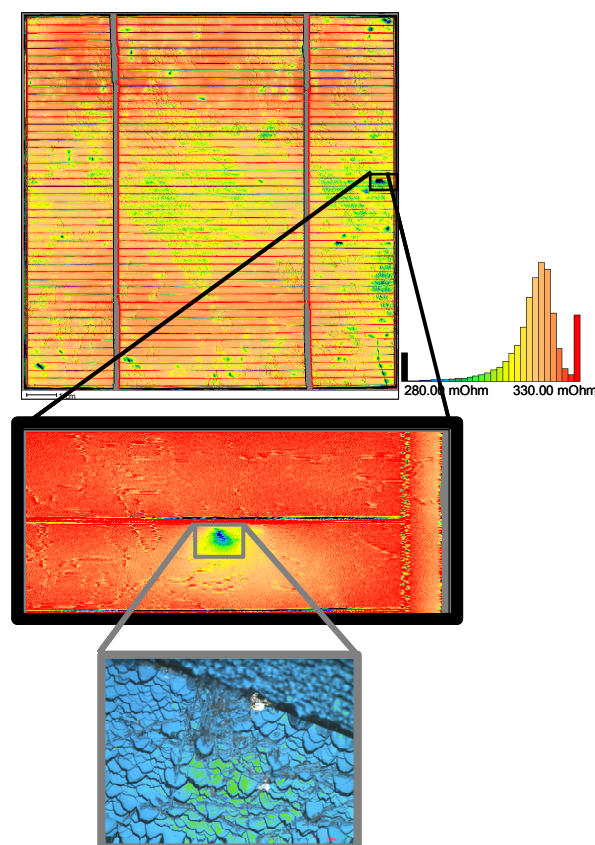


**Fig. 4:** Cell \_130:  $(dU_{\text{mpp}} / dI_{\text{sc}})$  with different scale: complete map (top), zoom map (black frame, middle); optical microscope image with  $\times 20$  magnification (grey frame, bottom).

#### 5 ACKNOWLEDGMENTS

We like to thank Jan-Martin Wagner for fruitful discussions.

#### 6 REFERENCES

- [1] S. Keipert, P. Wang, D. Borchert, S. Müller, L. Kühnemann, and M. Rinio, in *Proc. 23rd European Photovoltaic Solar Energy Conference*, 2CV.5.9, Valencia (2008).
- [2] H. Angermann, *Anal. Bioanal. Chem.* **374**, 676 (2002).
- [3] J. Carstensen, A. Schütt, and H. Föll, in *Proc. 23rd European Photovoltaic Solar Energy Conference*, 1CV.1.38, Valencia (2008).
- [4] J. Carstensen, A. Abdollahinia, A. Schütt, and H. Föll, in *Proc. 24th European Photovoltaic Solar Energy Conference*, 1CV.4.33, Hamburg (2009).
- [5] J. Carstensen, S. Mathijssen, G. Popkirov, and H. Föll, in *Proc. 20th European Photovoltaic Solar Energy Conference*, 1AV.2.40, Barcelona (2005).
- [6] M. Langenkamp and O. Breitenstein, *Solar Energy Materials & Solar Cells* **72**, 433 (2002).